J. Fluid Mech. (2019), *vol.* 875, R2, doi:10.1017/jfm.2019.545

JFM RAPIDS
journals.cambridge.org/rapids

Online *in situ* prediction of 3-D flame evolution from its history 2-D projections via deep learning

Jianqing Huang[1], **Hecong Liu**[1] **and Weiwei Cai**[1,†]

[1]Key Lab of Education Ministry for Power Machinery and Engineering, School of Mechanical Engineering, Shanghai Jiao Tong University, 800 Dongchuan Road, Shanghai 200240, China

(Received 6 May 2019; revised 28 June 2019; accepted 2 July 2019;
first published online 18 July 2019)

Online *in situ* prediction of 3-D flame evolution has been long desired and is considered to be the Holy Grail for the combustion community. Recent advances in computational power have facilitated the development of computational fluid dynamics (CFD), which can be used to predict flame behaviours. However, the most advanced CFD techniques are still incapable of realizing online *in situ* prediction of practical flames due to the enormous computational costs involved. In this work, we aim to combine the state-of-the-art experimental technique (that is, time-resolved volumetric tomography) with deep learning algorithms for rapid prediction of 3-D flame evolution. Proof-of-concept experiments conducted suggest that the evolution of both a laminar diffusion flame and a typical non-premixed turbulent swirl-stabilized flame can be predicted faithfully in a time scale on the order of milliseconds, which can be further reduced by simply using a few more GPUs. We believe this is the first time that online *in situ* prediction of 3-D flame evolution has become feasible, and we expect this method to be extremely useful, as for most application scenarios the online *in situ* prediction of even the large-scale flame features are already useful for an effective flame control.

Key words: computational methods, combustion, flames

1. Introduction

Flames are one of the most complex nonlinear dynamic systems, which involve the interplay between chemical reactions, heat and mass transfer, and flow dynamics (Sohn *et al.* 2000; Kashinath, Waugh & Juniper 2014). Since the eighteenth century, generations of scientists have devoted themselves to the study of flames, hoping to master the law of combustion and predict the evolution of practical flames. Even though considerable progress has been made due to the emergence of large-scale

† Email address for correspondence: cweiwei@sjtu.edu.cn

clusters and the development of computational fluid dynamics (CFD), online *in situ* prediction of 3-D flame evolution is still a formidable task (Kaminski *et al.* 2000; Klein, Chakraborty & Ketterl 2017), mainly for two reasons: first, CFD modelling involves the solution of Navier–Stokes equations with millions or even billions of cells and thousands of time steps; second, a detailed chemical kinetic mechanism is only available for simple low-carbon fuels (Curran 2019). In addition, since the CFD modelling is highly sensitive to boundary conditions – for example, the roughness and geometry of the boundary – this will cause extreme difficulties in practical applications where the boundary conditions are hard to define. Thus, the proposal and development of an alternative approach for 3-D flame prediction is of great interest.

Recently, time-resolved volumetric tomography (VT) for combustion diagnostics has made significant progress due to the invention of high-energy burst mode lasers and upgrades in high-speed cameras (Halls *et al.* 2017*a*, 2018). For example, volumetric imaging of important intermediate flame species such as OH, CH_2O and PAH has been demonstrated with a repetition rate up to 10 kHz (Halls *et al.* 2017*b*,*c*). The development of VT has greatly facilitated understanding of complex combustion processes such as flame ignition and combustion instability (Ma *et al.* 2016; Ruan *et al.* 2019). In addition, enormous amounts of experimental data can be accumulated within a short period of time. Such an amount of data provides unprecedented opportunities for machine learning (ML) algorithms which can effectively explore the hidden information behind the large dataset and make a faithful regression (Xu, Pei & Lai 2017) or prediction (Bakkouri & Afdel 2017). For example, in a recent review of developments in improving turbulence models by using ML algorithms it was proposed that data-driven approaches can be used to design useful predictive models (Duraisamy, Iaccarino & Xiao 2019). In particular, Kutz recommends that deep learning (DL) may play a key role in the field of fluid dynamics (Kutz 2017).

So far, successful applications of DL have been reported in various fields such as computer vision and speech recognition for its great ability to approximate complex functions of nonlinear systems (LeCun, Bengio & Hinton 2015). For example, convolution neural network (CNN) is famous for its capability in extracting features from images and has been applied extensively in medical imaging (Litjens *et al.* 2017), such as computed tomography (CT) and magnetic resonance imaging (MRI). In addition, DL algorithms had also been applied to predict heat release rates (Tóth, Garami & Csordás 2017; Wang, Song & Chen 2017), NO_x emission (Li *et al.* 2016) and oxygen contents (Yi, Yu & Chen 2017) for combustion studies. Long short-term memory (LSTM) neural network (Hochreiter & Schmidhuber 1997) is one such algorithm that excels in predicting time series data, such as stock markets (Nelson, Pereira & Oliveira 2017), weather forecasting (Qing & Niu 2018) and simulated turbulent flows (Alathur Srinivasan 2018; Mohan & Gaitonde 2018; Wang *et al.* 2018), to list a few. It has also been demonstrated for stance detection, where it has obtained state-of-the-art results (Augenstein *et al.* 2016).

In this work, we aim to develop a data-driven approach to predict 3-D flame evolution, which combines the state-of-the-art VT technique with DL algorithms. The former can provide a tremendous amount of useful experimental data and the latter can effectively utilize this big data to construct efficient neural networks for prediction. Different from the CFD approaches, which start from the Navier–Stokes equations, here we start directly from experimental data of the target flame measured at previous time instants. The advantage is obvious – our method starts from true representations of the practical flame; however, this is not necessarily guaranteed by a CFD technique, as it depends on how accurate the flow model and the chemical kinetic mechanisms are, and how well the initial conditions can be characterized.

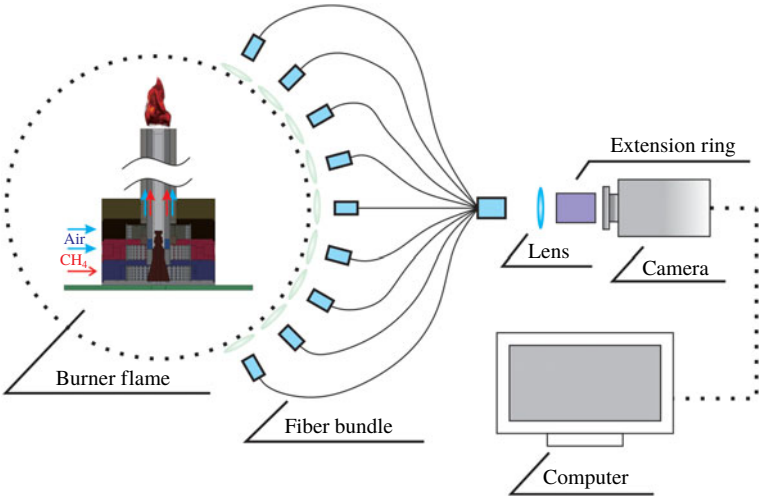

FIGURE 1. Illustration of the volumetric tomography system, which consists of one swirl-stabilized burner, one customized fibre bundle, one high-speed camera and one computer. Nine projections from different angles are captured simultaneously and then used for the reconstruction of 3-D flame structures to generate both the training and testing datasets.

2. Volumetric tomography of 3-D flame imaging

In this work, we designed a hybrid CNN–LSTM model to rapidly predict the evolution of 3-D flame structures based on its history 2-D projections without explicit tomographic reconstructions. Volumetric tomography of 3-D flame chemiluminescence was adopted here to generate a trustworthy dataset. The layout of the experimental set-up is shown in figure 1. Nine projections of the flame from different perspectives at each time instant were simultaneously captured by a camera through a customized fibre bundle which has nine input ends and one output end. The 3-D flame structures can then be reconstructed using the so-called algebraic reconstruction technique (ART) (Yu *et al.* 2018). More details about the VT system, including the components of the set-up as well as the reconstruction process, can be found in the supplementary material available at https://doi.org/10.1017/jfm.2019.545. Capturing the projections continuously, for example, for 10 s with a framing rate of 1k and repeating the reconstruction processes, a dataset including 10 000 consecutive frames of the 3-D flame structures can be obtained. To test the CNN–LSTM model, both a simple laminar diffusion flame (Flame no. 1, see figure 2(*a*)) and a complex non-premixed turbulent swirl-stabilized flame (Flame no. 2, see figure 2(*b*)) were tested, which contain the main features of flame evolution, including changing flame heights, drifting of flame wrinkles and the rotation of flames. As shown in the movie (see supplementary material), the profile of both flames changed considerably over time. For both Flame no. 1 and Flame no. 2, the reconstruction volume was discretized into $50 \times 50 \times 110$ voxels, with each voxel having dimensions of 0.5 mm $\times$ 0.5 mm $\times$ 0.5 mm.

To validate the correctness of the reconstructions, the re-projection method was applied (Yu *et al.* 2018). In this method, eight projections were used to reconstruct the 3-D flame structure, which was then used to predict the ninth projection. If the reconstruction is correct, then the estimate of the ninth projection should be

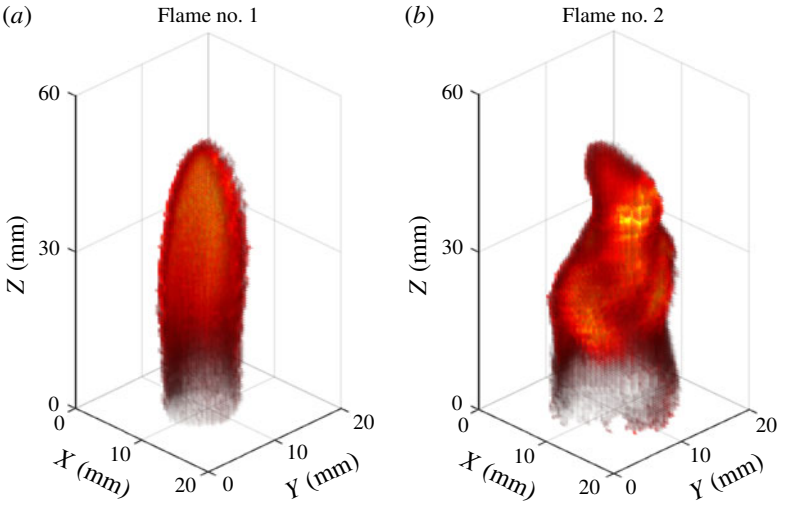

FIGURE 2. The 3-D renderings for Flame no. 1 and Flame no. 2.

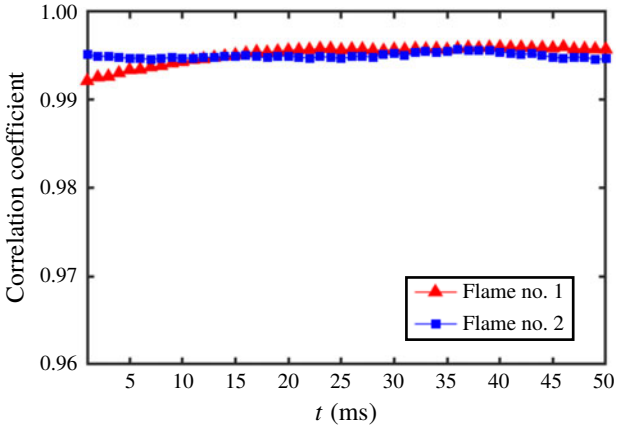

FIGURE 3. Correlation coefficients between the ninth measured projection and its corresponding re-projection, which are plotted as a function of the frame index of the two flames, respectively.

consistent with the measured one. The correlation coefficient (R) between the estimate and the measurement of the ninth projection was used to quantify the quality of reconstructions. The definition of R between two projections ($\boldsymbol{X}$) and ($\boldsymbol{Y}$) is (Shi, Liu & Yu 2010)

$$R(\boldsymbol{X}, \boldsymbol{Y}) = \frac{(\boldsymbol{X} \cdot \boldsymbol{Y}^{\mathrm{T}})}{\|\boldsymbol{X}\|_2 \times \|\boldsymbol{Y}\|_2}, \tag{2.1}$$

where $(\cdot)$ represents the dot product between two vectors, $\|\cdot\|_2$ is the 2-norm of the vector and superscript T means the transpose of the row vector. As shown in figure 3, the correlation coefficients are constantly larger than 0.99 for the selected 50 frames of both flames, suggesting a good reconstruction accuracy of the VT system. Thus,

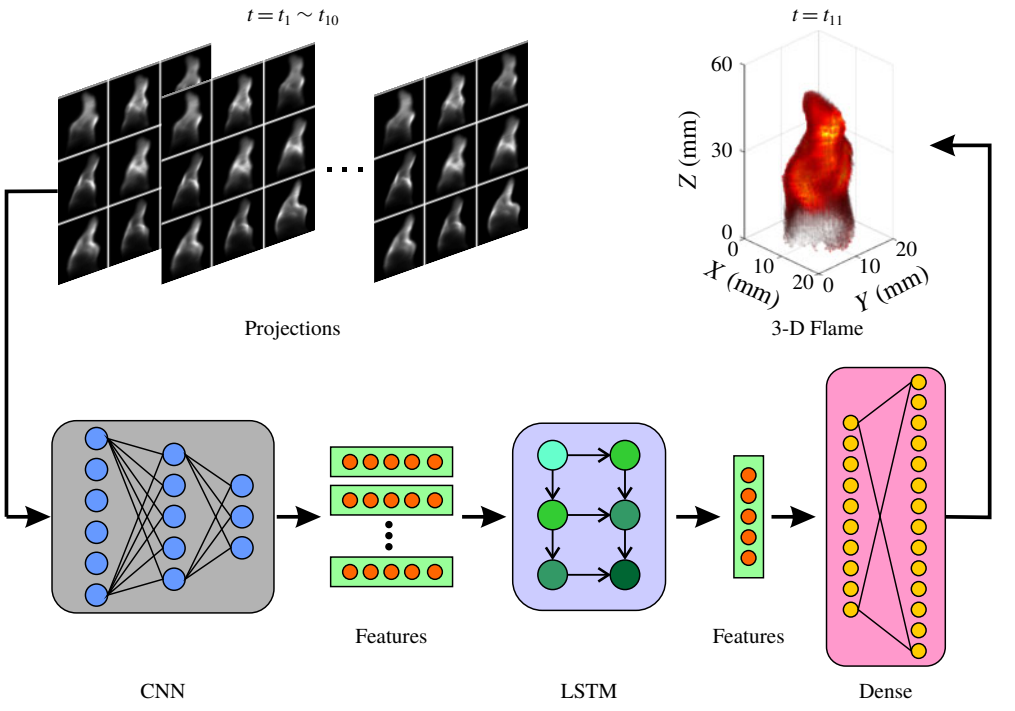

FIGURE 4. Schematic of the proposed CNN–LSTM model. The 3-D flame evolution (for example, $t = t_{11}$) can be predicted based on its history 2-D projections (for example, $t = t_1 \sim t_{10}$) using this model, which comprises a convolutional neural network (CNN), a long short-term memory network (LSTM) and a dense layer.

the reconstructions of the flames using the ART algorithm can be considered as the ground truths and used to train and test our CNN–LSTM model.

3. Deep neural network

The evolution of a 3-D flame structure is essentially composed of translation, rotation, scaling, erosion and dilation of the structure. These operations are elemental for image processing and can be learned effectively with a deep learning algorithm. The schematic of our CNN–LSTM model is illustrated in figure 4. First, 10 000 samples obtained from the VT measurements, each of which contains nine projections and the corresponding 3-D flame structure, were divided into five groups to perform 5-fold cross-validation for our model. For example, the first four groups, containing 8000 samples ($t = 0.001$ s $\sim$ 8.000 s), were used as the training dataset, and the last group, containing 2000 samples ($t = 8.001$ s $\sim$ 10.000 s), was used as the testing dataset. The results presented below are the average results from the 5-fold cross-validation. The detailed frameworks of CNN and LSTM as well as the training strategies can be found in the supplementary material.

It is noteworthy that the training process consists of two steps – training the CNN to extract features from projections, then training the LSTM to model the temporal sequence of these features. Within the iterations of the first step, nine projections at each time instant were put into CNN to obtain a vector of useful features. The 2-D projections for each frame can then be represented by the feature vector. Therefore,

the problem of predicting the 3-D flame evolution can be transformed into another one of predicting the evolution of the corresponding feature vectors. Within the iterations in the second step, a sequence of history feature vectors (for example, at $t = t_1 \sim t_h$) and a future one (for example, at $t = t_{h+\Delta t}$) were sent to the input layer and the output layer of the LSTM, respectively. The subscripts h and Δt denote history time window and prediction horizon, respectively. After 30 epochs, the loss function L2 converged and a trained CNN–LSTM prediction model was obtained. The details of the training process and the optimization of hyperparameters can be found in the supplementary material. Finally, the testing process was performed using the testing dataset. For instance, as shown in figure 4, projections ($t = t_1 \sim t_{10}$) in the testing dataset were input to the trained CNN–LSTM model to obtain the prediction of 3-D flame structure ($t = t_{11}$), that is, $h = 10$ ms and $\Delta t = 1$ ms, which can be treated as one testing case.

4. Results

The neural networks were implemented, trained and tested using Keras (version 2.22.4) using the TensorFlow backend (version 12.112.0) in Python (version 32.62.8). All algorithms were implemented on a workstation equipped with an Intel® Core2™ i7-DMI2-X79 PHC 2·60 GHz CPU with a single NVIDIA TITAN XP GPU with 12 GB VRAM. The training process of the CNN–LSTM model took approximately 30 min and the computational cost for each prediction was approximately 2 ms without any specific code optimization. Thus, online *in situ* prediction of 3-D flame evolution can be achieved with a moderate coding effort by using multiple GPUs for parallel computing (You *et al.* 2017). Hence, our proposed method has an overwhelming advantage in terms of computational efficiency compared with CFD techniques.

The testing results for three cases of both Flame no. 1 and no. 2 are shown in figures 5 and 6, respectively. As can be seen, there is almost no difference in the 3-D distributions between the ground truths (panels *a–c*) and the predictions (panels *d–f*), proving that our prediction model can successfully 'learn' the evolution law of flames and make accurate predictions. Furthermore, the middle slices of these 3-D distributions were selected to better illustrate the prediction performance of our proposed method, as shown in the last two rows of figures 5 and 6. As expected, the internal structures of both flames can be faithfully predicted as well. Thus, by using the CNN–LSTM model, the evolution of 3-D flame structures, including changing flame height, drifting of flame wrinkles and rotation of the flame, can be predicted accurately based on its history 2-D projections without explicitly tomographic reconstructions.

To further investigate the prediction capability of our CNN–LSTM model, several comparative experiments have been conducted with the same training and testing datasets. Quantitatively, the correlation coefficient (R) and the root mean square error (RMSE) between the predictions and the ground truths were adopted as the performance parameters to evaluate prediction accuracy. The testing results as a function of prediction horizon (Δt) are shown in figure 7. The values of R and RMSE remained nearly constant for Flame no. 1 (black lines) and changed slightly for Flame no. 2 (blue lines), when Δt increased from 5 ms to 30 ms. In contrast, the inherent R and RMSE between two consecutive true frames (that is, the ground truths) with the same time interval (Δt) were calculated as the basic benchmark. The results are shown in figure 7 (red and magenta lines for Flame no. 1 and Flame no. 2,

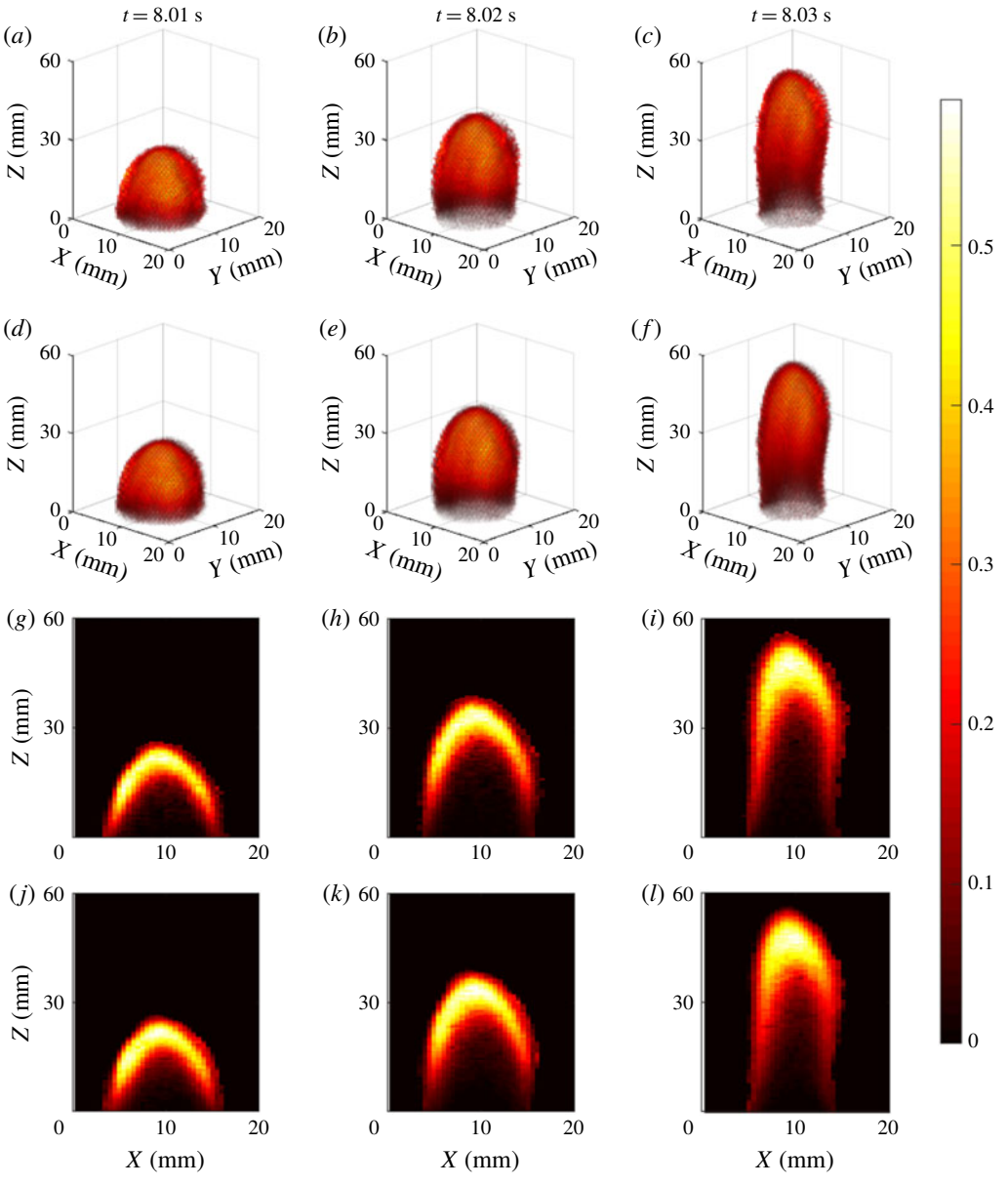

FIGURE 5. Prediction of Flame no. 1 using the CNN–LSTM model. Panels (*a–c*) are the ground truths at three time instants and panels (*d–f*) are the corresponding predictions obtained using the CNN–LSTM model. Panels (*g–l*) are the middle slices of panels (*a–f*), respectively.

respectively). Obviously, for the same Δt, the inherent difference between two ground truths is much larger than the difference between the prediction and the ground truth for both Flame no. 1 and Flame no. 2, indicating the effectiveness of prediction.

In addition, it has been found that the performance of the CNN–LSTM model varied for Flame no. 1 and Flame no. 2. This is mainly due to the distinct features

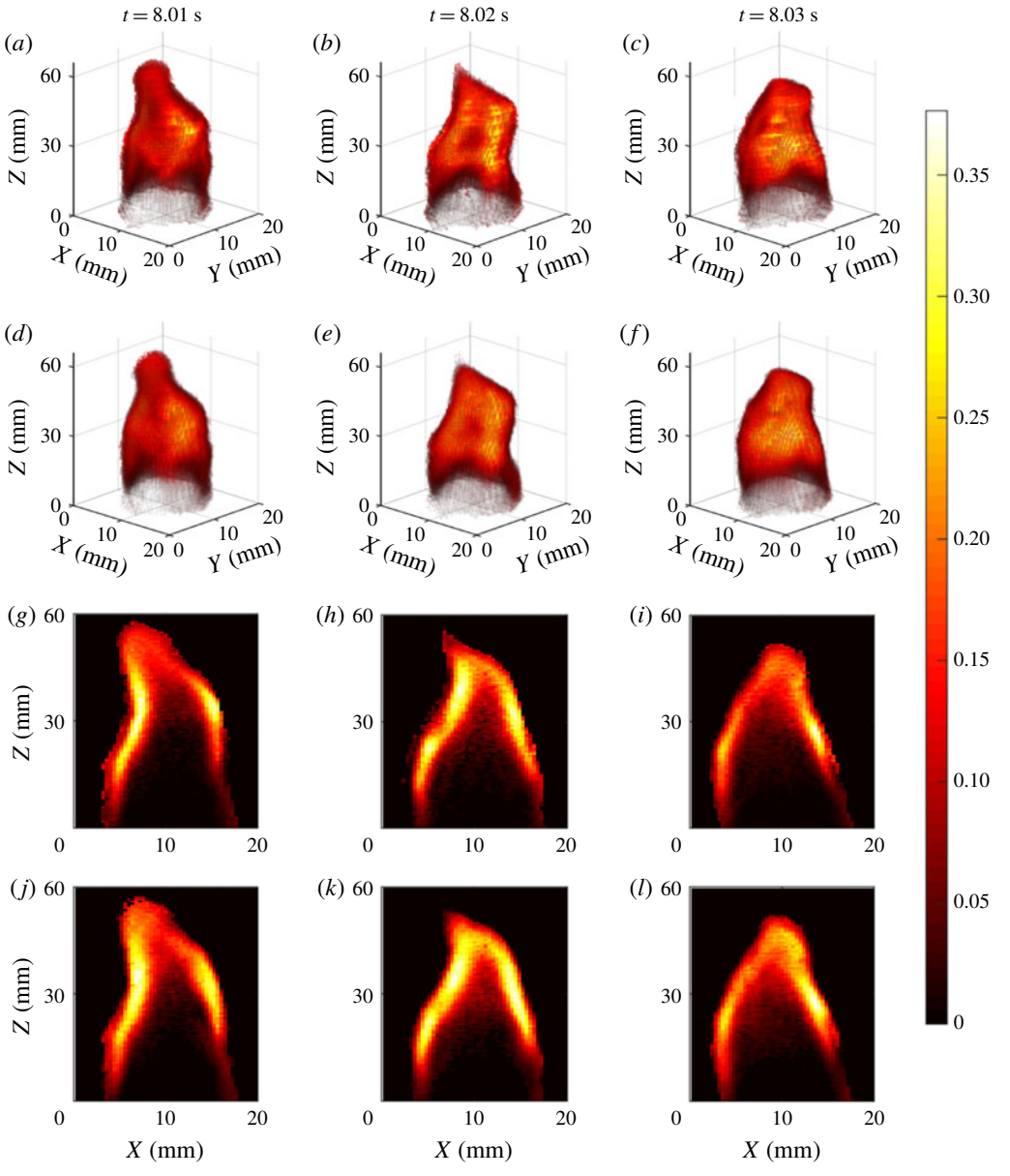

FIGURE 6. Prediction of Flame no. 2 using the CNN–LSTM model. Panels (*a–c*) are the ground truths at three time instants and panels (*d–f*) are the corresponding predictions obtained using the CNN–LSTM model. Panels (*g–l*) are the middle slices of panels (*a–f*), respectively.

of their structures and evolutions. Qualitatively, the evolution of Flame no. 1 was mainly reflected in the variation of the flame height, while the flame surface stayed relatively smooth over time. However, the height of Flame no. 2 was almost constant, but there were obvious wrinkles on the flame surface which drifted over time, making the flame structure more complicated. Its evolution is associated with vortex

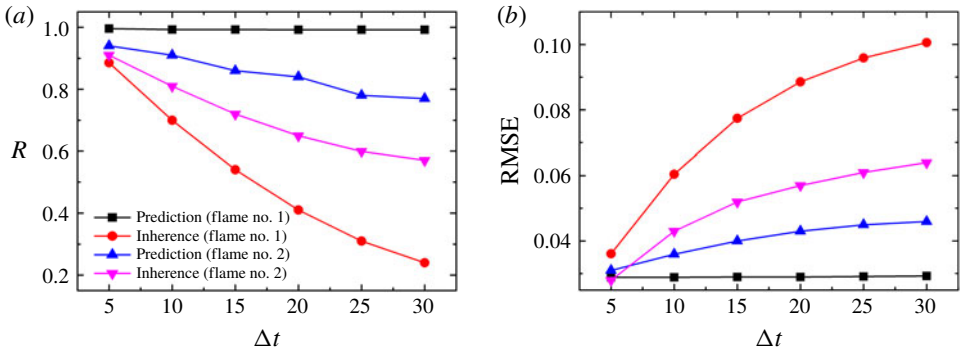

FIGURE 7. Performance of CNN–LSTM model. The black and blue lines indicate the prediction performance (R: correlation coefficient; RMSE: root mean square error) as a function of prediction horizon (Δt) for both Flame no. 1 and Flame no. 2. The red and magenta lines denote the inherent R and RMSE between two consecutive true frames (i.e. ground truths) with the same time interval (Δt).

generation, movement and shedding. According to a relevant CFD study (Hasegawa, Nakamichi & Nishiki 2002), small-scale vortices are more complex and irregular than large-scale vortices, and the evolution of Flame no. 2 was controlled by both scale vortices. To improve the prediction of Flame no. 2, more training samples should be incorporated so that more useful features of the small-scale vortices can be extracted, which is within the scope of our future research direction.

The successful demonstration of the CNN–LSTM model in predicting 3-D flame evolution suggested its potential for practical applications. In order to mimic the practical situations where measurement noise prevails, a series of experiments with different noise levels in projections were conducted. Additional artificial Gaussian noise was added to the measured projections as

$$p' = p \times (1 + \delta \times g),\ g \sim G(0, 1), \tag{4.1}$$

where p denotes the measured projections without noise, δ is the noise level and g is a set of random numbers that satisfy a Gaussian distribution. The results shown in figure 8 suggested good noise immunity of the proposed CNN–LSTM model.

5. Summary

To summarize, a data-driven approach for the online *in situ* prediction of 3-D flame evolution based on volumetric tomography and deep learning algorithms has been proposed. The method was successfully demonstrated with proof-of-concept experiments by predicting the evolution of both a laminar diffusion flame and a non-premixed turbulent swirl-stabilized flame. There are two key advantages of this prediction model. First, the model starts directly from the experimental data of the target flame measured at previous time instants, which are true representations of the practical flames. Second, unlike CFD techniques, the solution of a complicated partial differential equation system is not required and only simple algorithmic operations are involved, resulting in an overwhelming advantage over CFD techniques in terms of computational efficiency. Thus, it serves as a promising alternative approach to CFD techniques for applications where rapid prediction of 3-D flame evolution is required.

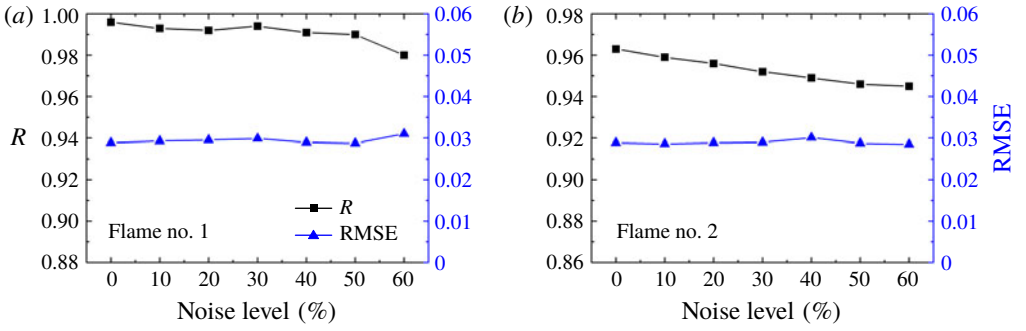

FIGURE 8. Results of experiments with different noise levels in projections. Additional artificial Gaussian noise was added to the measured projections to mimic the practical situations. Although the noise level increases gradually, R decreases slightly and the RMSE remains nearly constant for both Flame no. 1 and Flame no. 2.

Although there was an implicit assumption that the dominant flame features of the training dataset and the testing dataset are similar (Noack, Morzyski & Tadmor 2011), the prediction horizon can be effectively expanded when a larger training dataset is available. With the help of the proposed CNN–LSTM predictor, some key structure parameters of the flame (Floyd, Geipel & Kempf 2011) – such as flame surface density, wrinkling factor, flame normal direction and flame curvature, to name a few – can be calculated based on the predicted 3-D flame structures. Thus, these key parameters, which are related to flame stability and propagation (Floyd *et al.* 2011), can be used to control turbulent flames (Brunton & Noack 2015). Finally, the successful demonstration of our proposed model is just an example application of deep learning in predicting complex flows. It should be emphasized that this method can also be applied to predict the evolution of any other physical parameters/fields of reactive/non-reactive flows, such as the velocity field measured by particle image velocimetry (Baum *et al.* 2013) and the temperature field measured by two-line atomic fluorescence spectroscopy (Hult, Burns & Kaminski 2005; Fang *et al.* 2019).

Acknowledgements

This work was funded by the National Natural Science Foundation of China under grant no. 51706141.

Supplementary movies

Supplementary movies are available at https://doi.org/10.1017/jfm.2019.545.

References

ALATHUR SRINIVASAN, P. A. 2018 Deep learning models for turbulent shear flow. Thesis, KTH Royal Institute of Technology.

AUGENSTEIN, I., ROCKTÄSCHEL, T., VLACHOS, A. & BONTCHEVA, K. 2016 Stance detection with bidirectional conditional encoding. arXiv:1606.05464.

BAKKOURI, I. & AFDEL, K. 2017 Breast tumor classification based on deep convolutional neural networks. In *International Conference on Advanced Technologies for Signal & Image Processing*. IEEE.

BAUM, E., PETERSON, B., SURMANN, C., MICHAELIS, D., BÖHM, B. & DREIZLER, A. 2013 Investigation of the 3D flow field in an IC engine using tomographic PIV. *Proc. Combust. Inst.* **34** (2), 2903–2910.

BRUNTON, S. L. & NOACK, B. R. 2015 Closed-loop turbulence control: progress and challenges. *Appl. Mech. Rev.* **67** (5), 050801.

CURRAN, H. J. 2019 Developing detailed chemical kinetic mechanisms for fuel combustion. *Proc. Combust. Inst.* **37** (1), 57–81.

DURAISAMY, K., IACCARINO, G. & XIAO, H. 2019 Turbulence modeling in the age of data. *Annu. Rev. Fluid Mech.* **51**, 357–377.

FANG, B., ZHANG, Z., LI, G., TAO, B., WANG, S., HU, Z. & SONG, M. 2019 Simple calibrated nonlinear excitation regime two-line atomic fluorescence thermometry. *Opt. Lett.* **44** (2), 227–230.

FLOYD, J., GEIPEL, P. & KEMPF, A. M. 2011 Computed tomography of chemiluminescence (ctc): Instantaneous 3D measurements and phantom studies of a turbulent opposed jet flame. *Combust. Flame* **158** (2), 376–391.

HALLS, B. R., GORD, J. R., MEYER, T. R., THUL, D. J., SLIPCHENKO, M. & ROY, S. 2017*a* 20-kHz-rate three-dimensional tomographic imaging of the concentration field in a turbulent jet. *Proc. Combust. Inst.* **36** (3), 4611–4618.

HALLS, B. R., HSU, P. S., JIANG, N., LEGGE, E. S., FELVER, J. J., SLIPCHENKO, M. N., ROY, S., MEYER, T. R. & GORD, J. R. 2017*b* kHz-rate four-dimensional fluorescence tomography using an ultraviolet-tunable narrowband burst-mode optical parametric oscillator. *Optica* **4** (8), 897–902.

HALLS, B. R., HSU, P. S., ROY, S., MEYER, T. R. & GORD, J. R. 2018 Two-color volumetric laser-induced fluorescence for 3D OH and temperature fields in turbulent reacting flows. *Opt. Lett.* **43** (12), 2961–2964.

HALLS, B. R., JIANG, N., MEYER, T. R., ROY, S., SLIPCHENKO, M. N. & GORD, J. R. 2017*c* 4D spatiotemporal evolution of combustion intermediates in turbulent flames using burst-mode volumetric laser-induced fluorescence. *Opt. Lett.* **42** (14), 2830–2833.

HASEGAWA, T., NAKAMICHI, R. & NISHIKI, S. 2002 Mechanism of flame evolution along a fine vortex. *Combust. Theor. Model.* **6** (3), 413–424.

HOCHREITER, S. & SCHMIDHUBER, J. 1997 Long short-term memory. *Neural Comput.* **9** (8), 1735–1780.

HULT, J., BURNS, I. S. & KAMINSKI, C. F. 2005 Two-line atomic fluorescence flame thermometry using diode lasers. *Proc. Combust. Inst.* **30** (1), 1535–1543.

KAMINSKI, C. F., BAI, X. S., HULT, J., DREIZLER, A., LINDENMAIER, S. & FUCHS, L. 2000 Flame growth and wrinkling in a turbulent flow. *Appl. Phys.* B **71** (5), 711–716.

KASHINATH, K., WAUGH, I. C. & JUNIPER, M. P. 2014 Nonlinear self-excited thermoacoustic oscillations of a ducted premixed flame: bifurcations and routes to chaos. *J. Fluid Mech.* **761**, 399–430.

KLEIN, M., CHAKRABORTY, N. & KETTERL, S. 2017 A comparison of strategies for direct numerical simulation of turbulence chemistry interaction in generic planar turbulent premixed flames. *Flow Turbul. Combust.* **99** (3), 955–971.

KUTZ, J. N. 2017 Deep learning in fluid dynamics. *J. Fluid Mech.* **814**, 1–4.

LECUN, Y., BENGIO, Y. & HINTON, G. 2015 Deep learning. *Nature* **521** (7553), 436–444.

LI, N., LU, G., LI, X. & YAN, Y. 2016 Prediction of NO_x emissions from a biomass fired combustion process based on flame radical imaging and deep learning techniques. *Combust. Sci. Technol.* **188** (2), 233–246.

LITJENS, G., KOOI, T., BEJNORDI, B. E., SETIO, A. A. A., CIOMPI, F., GHAFOORIAN, M., VAN DER LAAK, J. A. W. M., VAN GINNEKEN, B. & SÁNCHEZ, C. I. 2017 A survey on deep learning in medical image analysis. *Med. Image Anal.* **42**, 60–88.

MA, L., LEI, Q., WU, Y., XU, W., OMBRELLO, T. M. & CARTER, C. D. 2016 From ignition to stable combustion in a cavity flameholder studied via 3D tomographic chemiluminescence at 20 kHz. *Combust. Flame* **165**, 1–10.

MOHAN, A. T. & GAITONDE, D. V. 2018 A deep learning based approach to reduced order modeling for turbulent flow control using LSTM neural networks. arXiv:1804.09269.

NELSON, D. M. Q., PEREIRA, A. C. M. & OLIVEIRA, R. A. D. 2017 Stock market's price movement prediction with LSTM neural networks. In *Intl Joint Conference on Neural Networks*, pp. 1419–1426. IEEE.

NOACK, B. R., MORZYSKI, M. & TADMOR, G. 2011 *Reduced-Order Modelling for Flow Control*. Springer.

QING, X. & NIU, Y. 2018 Hourly day-ahead solar irradiance prediction using weather forecasts by LSTM. *Energy* **148**, 461–468.

RUAN, C., YU, T., CHEN, F., WANG, S., CAI, W. & LU, X. 2019 Experimental characterization of the spatiotemporal dynamics of a turbulent flame in a gas turbine model combustor using computed tomography of chemiluminescence. *Energy* **170**, 744–751.

SHI, L. L., LIU, Y. Z. & YU, J. 2010 PIV measurement of separated flow over a blunt plate with different chord-to-thickness ratios. *J. Fluids Struct.* **26** (4), 644–657.

SOHN, C. H., KIM, J. S., CHUNG, S. H. & MARUTA, K. 2000 Nonlinear evolution of diffusion flame oscillations triggered by radiative heat loss. *Combust. Flame* **123** (1), 95–106.

TÓTH, P., GARAMI, A. & CSORDÁS, B. 2017 Image-based deep neural network prediction of the heat output of a step-grate biomass boiler. *Appl. Energy* **200**, 155–169.

WANG, Z., SONG, C. & CHEN, T. 2017 Deep learning based monitoring of furnace combustion state and measurement of heat release rate. *Energy* **131**, 106–112.

WANG, Z., XIAO, D., FANG, F., GOVINDAN, R., PAIN, C. C. & GUO, Y. 2018 Model identification of reduced order fluid dynamics systems using deep learning. *Intl J. Numer. Meth. Fluids* **86** (4), 255–268.

XU, Y., PEI, J. & LAI, L. 2017 Deep learning based regression and multi-class models for acute oral toxicity prediction with automatic chemical feature extraction. *J. Chem. Inform. Model* **57** (11), 2672–2685.

YI, L., YU, F. & CHEN, J. 2017 Flame images for oxygen content prediction of combustion systems using DBN. *Energy Fuels* **31** (8), 8776–8783.

YOU, Y., ZHANG, Z., HSIEH, C. J., DEMMEL, J. & KEUTZER, K. 2017 ImageNet training in minutes. In *47th International Conference on Parallel Processing*. ACM.

YU, T., RUAN, C., LIU, H., CAI, W. & LU, X. 2018 Time-resolved measurements of a swirl flame at 4 kHz via computed tomography of chemiluminescence. *Appl. Opt.* **57** (21), 5962–5969.